

Lattice instabilities of cubic NiTi from first principles

Xiangyang Huang, Claudia Bungaro, Vitaliy Godlevsky and Karin M. Rabe

Department of Physics and Astronomy, Rutgers University, Piscataway, NJ 08854-8019

(November 5, 2018)

Abstract

The phonon dispersion relation of NiTi in the simple cubic $B2$ structure is computed using first-principles density-functional perturbation theory with pseudopotentials and a plane-wave basis set. Lattice instabilities are observed to occur across nearly the entire Brillouin zone, excluding three interpenetrating tubes of stability along the (001) directions and small spheres of stability centered at R. The strongest instability is that of the doubly degenerate $M_{5'}$ mode. The atomic displacements of one of the eigenvectors of this mode generate a good approximation to the observed $B19'$ ground-state structure.

I. INTRODUCTION

The realization of the technological promise of active materials in general, and shape memory alloys in particular, requires significant progress in the fundamental understanding of their nature and behavior. The relative chemical and structural simplicity of the shape memory alloy NiTi has made it a popular subject of both experimental and theoretical study¹.

The monoclinic *B19'* low-temperature structure of NiTi is related to the cubic *B2* high-temperature structure by approximately rigid shifts of alternate (110) planes along the (1 $\bar{1}$ 0) direction, resulting in a lowering of the symmetry and a corresponding change in the shape of the unit cell². Previous first-principles studies have focused on accurate prediction of the ground-state structural parameters by relaxing forces and stresses for a particular choice of space group, complementing the experimental structural determination data^{3,4}.

The distortion that relates the two structures has the symmetry of a single M-point normal mode of the *B2* structure. This suggests a parallel between the martensitic transformation from the *B2* to the *B19'* structure in NiTi and the paraelectric-ferroelectric “soft-mode” transition in perovskite oxides such as PbTiO₃, BaTiO₃ and KNbO₃⁵. In these perovskites, first-principles calculation of the eigenfrequencies and eigenvectors of the unstable phonons of the cubic high-symmetry prototype structure^{6–8} has shown that an excellent approximation to the ferroelectric ground-state structure is obtained by “freezing in” the single dominant unstable phonon (a polar optic mode at the zone center) with an accompanying change in the shape of the unit cell. The q-dependence of the instability across the Brillouin zone has been shown to determine the nature of local structural fluctuations in the high-temperature cubic paraelectric phase⁷ and, through a first-principles effective Hamiltonian analysis, the transition temperature and related quantities⁸.

In this paper, we take the first step in extending this approach to shape memory alloys by computing the phonon eigenfrequencies and eigenvectors of the cubic high-symmetry prototype structure of NiTi from first principles, as described in Section II. In Section

III, the dominant unstable phonon is identified and the structure it generates is compared with available knowledge of the ground state structure. We then investigate how these instabilities extend across the Brillouin zone. We conclude by speculating on the implications of this observation on the structure and properties of the high-temperature phase and on the martensitic transition.

II. COMPUTATIONAL METHOD

First-principles calculations of the structural energetics of *B2* NiTi were carried out within density-functional theory with a plane-wave pseudopotential approach. Phonon eigenfrequencies and eigenvectors throughout the Brillouin zone were obtained using the Green's function formulation of density-functional perturbation theory (DFPT)⁹. The calculations were performed with the PWSCF and PHONON codes¹⁰, using the Perdew-Zunger¹¹ parametrization of the local-density approximation (LDA). Ultrasoft pseudopotentials¹² for Ti and Ni were generated according to a modified Rappe-Rabe-Kaxiras-Joannopoulos (RRKJ) scheme¹³ with three Bessel functions¹⁴. The electronic wave functions were represented in a plane-wave basis set with a kinetic energy cutoff of 30 Ry. The augmentation charges were expanded up to 660 Ry. The Brillouin zone (BZ) integrations were carried out by the Hermite-Gaussian smearing technique¹⁵ using a 56 k-point mesh (corresponding to $12 \times 12 \times 12$ regular divisions along the k_x , k_y and k_z axes) in the $\frac{1}{48}$ irreducible wedge. The value of the smearing parameter was $\sigma=0.02$ Ry. These parameters yield phonon frequencies converged within 5 cm^{-1} . The dynamical matrix was computed on a $6 \times 6 \times 6$ q-point mesh commensurate with the k-point mesh. The complete phonon dispersion relation was obtained through the computation of real-space interatomic force constants within the corresponding box¹⁶.

In Table I, we report the equilibrium lattice parameter and elastic constants of *B2* NiTi obtained from pseudopotential total energy calculations performed as described above, and from a previous pseudopotential calculation using a mixed basis set(MB)³. For comparison,

we also performed full-potential linearized-augmented-plane-wave calculations (FLAPW) within both the LDA and the generalized-gradient approximation (GGA)¹⁷. The lattice parameter and bulk moduli were obtained from a Birch function fit²⁰. The discrepancy between the PWSCF and FLAPW values for the LDA lattice parameter is comparable ($< 1\%$) to that between the two pseudopotential results. The FLAPW lattice parameter is slightly larger within GGA, as expected, and the bulk moduli show the typical decrease with increasing lattice parameter. Although these results are not directly comparable with the properties of the entropically-stabilized high-temperature $B2$ phase, characterized by large fluctuating atomic displacements, the experimental data included in Table I are in general agreement with the first-principles values. The DFPT calculations reported in the next section were performed at the PWSCF lattice parameter 5.594 a.u.

III. RESULTS AND DISCUSSION

The full phonon dispersion of $B2$ NiTi consists of six branches: three acoustic and three optic. Results of our calculations along the high-symmetry lines of the simple cubic BZ are shown in Figure 1. The imaginary frequencies of the unstable modes are represented as negative values. The values of the phonon frequencies at the symmetry points are also listed in Table II. All of the eigenvectors at the symmetry points Γ , X, M and R are uniquely determined by symmetry considerations except for the $M_{5'}$ modes, to be discussed in more detail below.

As expected on the basis of experimental observation of the low-temperature structure, the $B2$ structure is unstable at $T = 0$. The dominant instability is a doubly-degenerate $M_{5'}$ mode. Since there is a second $M_{5'}$ mode (at high frequency), the atomic displacements corresponding to the unstable $M_{5'}$ mode are not uniquely determined by symmetry, but can be obtained only by diagonalizing the computed dynamical matrix. In addition, since the mode is doubly degenerate, there is a two-dimensional space of phonon eigenvectors that all correspond to the same frequency. Two particularly symmetrical eigenvectors in this space

are shown in Figure 2. In fact, the distorted structure produced by freezing the eigenvector in Figure 2(a) into the reference cubic structure yields, with an appropriate choice of overall amplitude, an excellent approximation to the observed ground-state $B19'$ structure. As can be seen in Table III, the main difference is in the angle γ , lowering the symmetry from orthorhombic to monoclinic. Energetically, this eigenvector is singled out from the others in this space not at quadratic order, but as the result of higher order terms, including strain coupling, not reported here. Detailed calculations will be presented in a future publication.

While the evolution of the lattice instability away from the zone center cannot be directly obtained experimentally, Figure 1 shows that the unstable phonon branches actually extend throughout the Brillouin zone. From the M point, the instability extends more than half of the way to Γ and X. At Γ , the acoustic branches behave normally at very small q . As q increases along Γ -R and Γ -M, one and two individual optic modes, respectively, disperse strongly downward, mixing with the acoustic branches and then becoming unstable. As the R point is approached along Γ -R, the unstable longitudinal mode turns around and becomes stable once again. Along Γ -X the Δ_1 optic mode similarly disperses downward and mixes with the Δ_1 acoustic branch, although along this line all phonon modes remain stable.

This behavior can be better visualized in a three-dimensional view of the BZ showing the $\omega^2=0$ isosurface (Figure 3). The region of stability is confined to three interpenetrating tubes along the cartesian axes, with additional bulges in the central region along the Γ -R directions, and to small approximately spherical regions around the R points. The unstable modes at M are thus continuously connected to the unstable mode along Γ -R.

Phonon frequencies along symmetry lines in the high-temperature $B2$ phase have been experimentally measured²³ and theoretically analyzed²⁴. As explained in Section II, the properties of this phase are not directly comparable with calculations for the unstable zero-temperature $B2$ structure (note, however, that the calculated stable acoustic mode frequencies are in general agreement with their experimental counterparts). The high-temperature $B2$ structure is entropically stabilized and should have strong local distortions away from the high-symmetry average positions of the atoms. As in the previous work on KNbO_3 , the na-

ture of these distortions should be related to the distribution of unstable modes in the BZ, and could be experimentally characterized through diffuse X-ray scattering or with local probes, such as EXAFS. The soft-mode behavior of NiTi is also less straightforward than that of the ferroelectric perovskites. In the cubic phase, a soft TA mode at $q = \frac{2\pi}{a_0}(\frac{1}{3}\frac{1}{3}0)$ freezes in to generate the intermediate-temperature R phase, and a softening of the $M_{5'}$ phonon associated with the ground-state B19' phase has not been directly observed. Theoretical investigation of the phase diagram and temperature-dependence of the phonon dispersion requires a first-principles effective Hamiltonian analysis, analogous to that for the perovskite oxides, beyond the scope of the present paper.

IV. CONCLUSIONS

In conclusion, we performed *ab initio* calculations of the phonon dispersion of the *B2* high-symmetry reference structure of NiTi. There are lattice instabilities throughout the entire Brillouin zone, with the dominant instability at M. A good approximation to the observed ground state structure of NiTi can be generated by freezing in a particular choice of eigenvector from the corresponding two-dimensional space.

ACKNOWLEDGMENTS

We thank R. D. James, K. Bhattacharya and I. I. Naumov for valuable discussions. This work was supported by AFOSR/MURI F49620-98-1-0433. A portion of the calculations were performed on the SGI Origin 2000 at ARL MSRC.

REFERENCES

- ¹ R. D. James and K. F. Hane, *Acta Mater.* **48**, 197 (2000).
- ² R. F. Hehemann and G. D. Sandrock, *Scr. Metall.* **5**, 801 (1971).
- ³ Y. Y. Ye, C. T. Chan, and K. M. Ho, *Phys. Rev. B* **56**, 3678 (1997).
- ⁴ M. Sanati, R. C. Albers, and F. J. Pinski, *Phys. Rev. B* **58**, 13590 (1998).
- ⁵ M. E. Lines and A. M. Glass, *Principles and Applications of Ferroelectrics and Related Materials* (Clarendon Press, Oxford, 1977).
- ⁶ Ph. Ghosez, E. Cockayne, U. V. Waghmare, and K. M. Rabe, *Phys. Rev. B* **60**, 836 (1999).
- ⁷ R. Yu and H. Krakauer, *Phys. Rev. Lett.* **74**, 4067 (1995).
- ⁸ U. V. Waghmare and K. M. Rabe, *Phys. Rev. B* **55**, 6161 (1997).
- ⁹ N. E. Zein, *Sov. Phys. Solid State* **26**, 1825 (1984); S. Baroni, P. Giannozzi, and A. Testa, *Phys. Rev. Lett.* **58**, 1861 (1987).
- ¹⁰ S. Baroni, S. de Gironcoli, A. Dal Corso, and P. Giannozzi, <http://www.sissa.it/cm/PWcodes>.
- ¹¹ J. P. Perdew and A. Zunger, *Phys. Rev. B* **23**, 5048 (1981).
- ¹² D. Vanderbilt, *Phys. Rev. B* **41**, 7892 (1990).
- ¹³ A. M. Rappe, K. M. Rabe, E. Kaxiras, and J. D. Joannopoulos, *Phys. Rev. B* **41**, 1227 (1990). 8245 (1994).
- ¹⁴ A. DalCorso, A. Pasquarello and A. Baldereschi, *Phys. Rev. B* **56**, 11369 (1997).
- ¹⁵ M. Methfessel and A. T. Paxton, *Phys. Rev. B* **40**, 3616 (1989).
- ¹⁶ P. Giannozzi, S. de Gironcoli, P. Pavone and S. Baroni, *Phys. Rev. B* **43**, 7231 (1991).
- ¹⁷ P. Blaha, K. Schwarz, and J. Luitz, WIEN97, Vienna University of Technology, Vienna

1997. (Improved and updated Unix version of the original copyrighted WIEN-code, published by P. Blaha, K. Schwarz, P. Sorantin, and S. B. Trickey, in Comput. Phys. Commun. **59**, 399 1990). Our FLAPW calculations were performed using a 56 k-point mesh in the $\frac{1}{48}$ irreducible wedge. No shape approximations were made to the density or potential. A $R_{MT}K_{MAX}$ of 11 were used. The Gaussian smearing method with a width of 0.001 Ry was used in the Brillouin zone integrations.
- ¹⁸ E. Goo and R. Sinclair, Acta Metall. **33**, 1717 (1985); K. Otsuka, T. Sawamura, and K. Shimizu, Phys. Status Solidi A **5**, 457 (1971).
- ¹⁹ O. Mercier, K. N. Melton, G. Gremand, and J. Hägi, J. Appl. Phys. **51**(3), 1833 (1980).
- ²⁰ F. Birch, J. Geophys. Res. **83**, 1257 (1978).
- ²¹ F. Bassani and G. Pastori Parravicini, *Electronic states and optical transitions in solids*, ed. by R. A. Ballinger (Oxford, New York, Pergamon Press, 1975).
- ²² Y. Kudoh, M. Tokonami, S. Miyazaki, and K. Otsuka, Acta Metall. Mater. **33**, 2049 (1985).
- ²³ H. Tietz, M. Müllner, and B. Renker, J. Phys. C **17**, L529 (1984).
- ²⁴ G. L. Zhao and B. N. Harmon, Phys. Rev. B **48**, 2031 (1993).

FIGURES

FIG. 1. Phonon dispersion for NiTi in the $B2$ structure with $a_0 = 5.594$ a.u. along symmetry lines in the simple cubic BZ. Symmetry labels are assigned according to the conventions of Ref. 21 with Ni at the origin. The imaginary frequencies of the unstable modes are plotted as negative values.

FIG. 2. Relative atomic displacements corresponding to two linearly independent eigenvectors of the unstable M'_5 mode at $\vec{k} = \frac{2\pi}{a_0}(\frac{1}{2}\frac{1}{2}0)$, transforming as (a) $\hat{x} + \hat{y}$ and (b) \hat{y} . Here, a portion of the $B2$ structure, with Ni atoms shown by filled circles and Ti atoms shown by open circles, is viewed along the (001) direction. All displacements lie in the x-y plane.

FIG. 3. Zero-frequency isosurfaces of the phonon dispersion relation in the first octant of the Brillouin zone. Outside the interpenetrating tubes along the (001) directions and the small spheres centered at R.

TABLES

TABLE I. Lattice parameter and elastic properties of NiTi in the $B2$ structure. a_0 in the parenthesis is GGA result.

	PW	MB(Ref. 3)	FLAPW ^a	Exp.
a_0 (a.u.)	5.594	5.626	5.561(5.670)	5.698(Ref. 18)
B(Mbar)	1.68	1.56	1.86	1.40(Ref. 19)
c_{11} (dyn/cm ²)	1.80	1.68	-	1.62(Ref. 19)
c_{12} (dyn/cm ²)	1.68	1.44	-	1.29(Ref. 19)
c_{44} (dyn/cm ²)	0.77	0.50	-	0.35(Ref. 19)

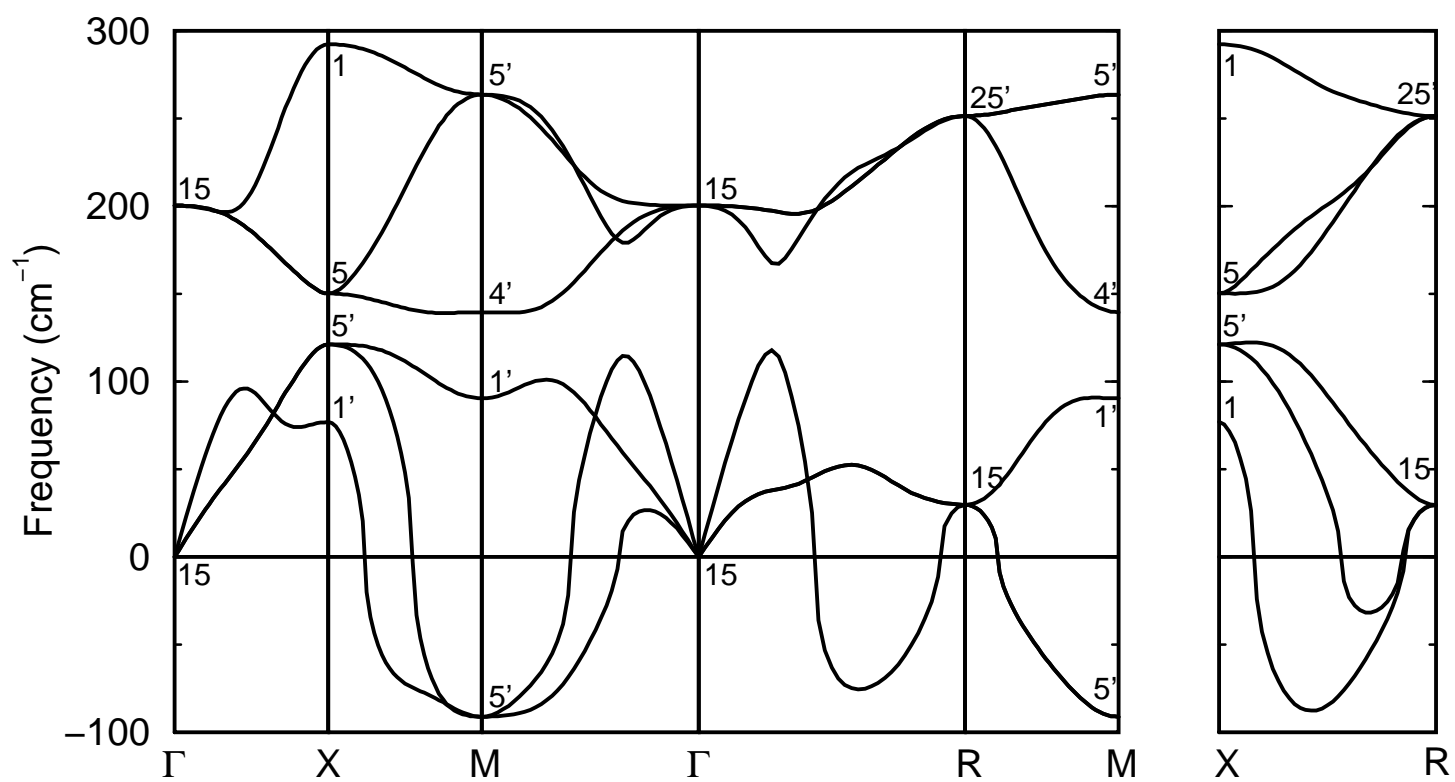
^aThis work. see Ref. 17

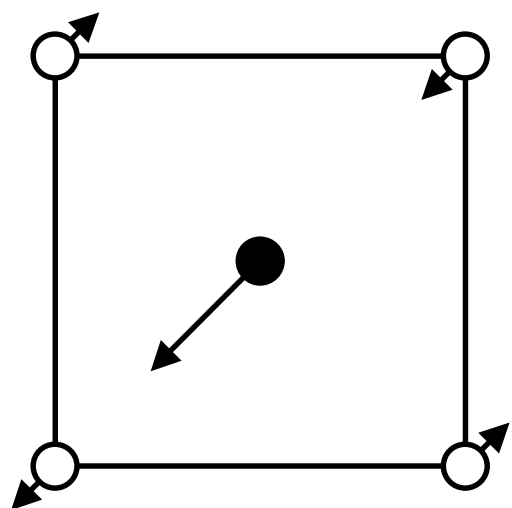
TABLE II. Computed phonon frequencies of $B2$ NiTi with $a_0 = 5.594$ a.u. at the symmetry points in the simple cubic BZ.

Label	Frequency(cm ⁻¹)	Label	Frequency(cm ⁻¹)
Γ_{15}	0	R_{15}	30
Γ_{15}	200	R_{25}	252
$X_{1'}$	77	$M_{5'}$	91 <i>i</i>
$X_{5'}$	121	$M_{1'}$	91
X_5	150	$M_{4'}$	140
X_1	293	$M_{5'}$	264

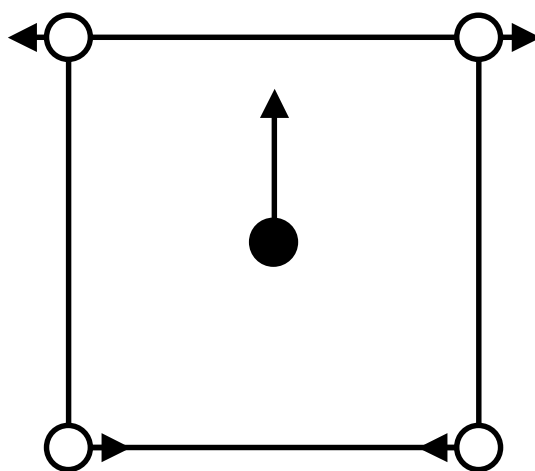
TABLE III. Structural parameters of $B2$ NiTi distorted by freezing in of the eigenvector in Figure 2, $a=2.960$ Å, $b=4.186$ Å, $c=4.186$ Å, $\gamma=90^\circ$, compared with the experimental monoclinic $B19'$ structure(Ref. 22), $a=2.898$ Å, $b=4.646$ Å, $c=4.108$ Å, $\gamma=97.78^\circ$. While the distorted $B2$ structure actually has space group $Pmma$, the structure is presented within $P2_1/m$, the space group of the $B19'$ structure, to facilitate comparison.

Structure	Wyckoff position	x	y	z
distorted $B2$	Ti(2e)	0.5	0.222	0.25
	Ni(2e)	0	0.678	0.25
$B19'$	Ti(2e)	0.4176	0.2164	0.25
	Ni(2e)	0.0372	0.6752	0.25





(a)



(b)

○ Ti

● Ni

